High-throughput assessment of hemoglobin polymer in single red blood cells from sickle cell patients under controlled oxygen tension

Giuseppe Di Caprio[a,b,c,1], Ethan Schonbrun[a,1], Bronner P. Gonçalves[a,d,e], Jose M. Valdez[f], David K. Wood[f,2], and John M. Higgins[a,d,e,2]

[a]Center for Systems Biology, Massachusetts General Hospital, Boston, MA 02114; [b]Program in Cellular and Molecular Medicine, Boston Children's Hospital, Boston, MA 02115; [c]Department of Cell Biology, Harvard Medical School, Boston, MA 02115; [d]Department of Pathology, Massachusetts General Hospital, Boston, MA 02114; [e]Department of Systems Biology, Harvard Medical School, Boston, MA 02115; and [f]Deparment of Biomedical Engineering, University of Minnesota, Minneapolis, MN 55455

Edited by William A. Eaton, National Institutes of Health, Bethesda, MD, and approved October 30, 2019 (received for review August 13, 2019)

Sickle cell disease (SCD) is caused by a variant hemoglobin molecule that polymerizes inside red blood cells (RBCs) in reduced oxygen tension. Treatment development has been slow for this typically severe disease, but there is current optimism for curative gene transfer strategies to induce expression of fetal hemoglobin or other nonsickling hemoglobin isoforms. All SCD morbidity and mortality arise directly or indirectly from polymer formation in individual RBCs. Identifying patients at highest risk of complications and treatment candidates with the greatest curative potential therefore requires determining the amount of polymer in individual RBCs under controlled oxygen. Here, we report a semiquantitative measurement of hemoglobin polymer in single RBCs as a function of oxygen. The method takes advantage of the reduced oxygen affinity of hemoglobin polymer to infer polymer content for thousands of RBCs from their overall oxygen saturation. The method enables approaches for SCD treatment development and precision medicine.

sickle cell disease | hemoglobin polymerization | erythrocytes | oxygen affinity | diagnostics

Sickle cell disease (SCD) is a blood disorder that affects millions worldwide. About 300,000 infants are born with the disease per year. All disease pathology is ultimately caused by polymerization of variant sickle hemoglobin (HbS) molecules in individual red blood cells (RBCs) under conditions of reduced oxygen tension. Polymerization of HbS inside RBCs immediately compromises RBC morphology and blood rheology, and it also triggers longer-term increase in inflammation and cellular adhesion, ultimately leading to ischemia, vaso-occlusion, stroke, tissue damage, and acute and chronic organ dysfunction. Sickle cell disease has a variable clinical course for patients, with some having very severe outcomes and some having more benign (1). Despite decades of research, we have limited understanding of the reasons for this variability, and efforts to find useful genotypic or clinical predictors of benign prognosis have been unsuccessful, leaving us with no useful in vitro biomarkers (2). Fetal hemoglobin (HbF) can inhibit polymer formation, and experience with patients with genetic variants and patients who respond to hydroxyurea treatment by up-regulating fetal hemoglobin shows that patient outcomes can be improved by reducing the amount of hemoglobin polymer that will form in individual RBCs at a given oxygen tension (3–6).

The prospects for improvement in sickle cell treatments have increased dramatically in recent years with several different approaches in advanced clinical trials, and at least 2 reports of individuals treated with different experimental gene transfer strategies, some of whom have remained disease-free more than a year after treatment (7–9). While these preliminary individual results are promising, it is not clear whether they will generalize. It is also not clear which new treatment strategies will work best for which patients, and we currently have no practical method to compare their efficacies. Most new treatment approaches share the same basic mechanism of action: reduce the fraction of circulating RBCs in which significant amounts of HbS will polymerize at physiologic oxygen tensions. Despite the excitement around these new experimental therapies, we still lack a method to measure Hb polymer in single RBCs and, thus, are unable to define therapeutic windows. We are therefore unable to optimize delivery of a particular therapy, and we have no accurate way to compare and prioritize these experimental treatments. Most importantly, we are left to manage patients with crude and imprecise biomarkers (2).

We previously reported a platform capable of directly measuring the hemoglobin-oxygen saturation of individual RBCs (10, 11). We have applied that method here to develop a semiquantitative measurement of Hb polymer in single RBCs under controlled oxygen tension. This method infers the presence of intracellular polymerized HbS from the polymer's effect of lowering the RBC's overall hemoglobin-oxygen saturation. As Fig. 1*A* illustrates, at a given oxygen tension, RBCs containing high amounts of Hb polymer will have lower hemoglobin-oxygen saturation than RBCs

Significance

Sickle cell disease is the first "molecular disease" described more than 100 years ago. All morbidity and mortality are ultimately caused by polymerization of the variant sickle hemoglobin molecule in red blood cells (RBCs). However, despite decades of intense research, we are unable to measure the amount of hemoglobin polymer in individual RBCs with high throughput at arbitrary oxygen tension. We describe a high-throughput method to assess hemoglobin polymer at the single-cell level under controlled oxygen tension. The assay infers hemoglobin polymer fraction by measuring its effect on cellular oxygen affinity. This method provides biomarkers promising to improve management of sickle cell patients and to optimize the development and prioritization of candidate cures.

Author contributions: G.D.C., E.S., B.P.G., D.K.W., and J.M.H. designed research; G.D.C., E.S., B.P.G., D.K.W., and J.M.H. performed research; J.M.V. contributed new reagents/analytic tools; G.D.C., E.S., B.P.G., D.K.W., and J.M.H. analyzed data; and G.D.C., E.S., B.P.G., D.K.W., and J.M.H. wrote the paper.

The authors declare no competing interest.

This article is a PNAS Direct Submission.

[1]G.D.C. and E.S. contributed equally to this work.

[2]To whom correspondence may be addressed. Email: dkwood@umn.edu or john_higgins@hms.harvard.edu.

This article contains supporting information online at https://www.pnas.org/lookup/suppl/doi:10.1073/pnas.1914056116/-/DCSupplemental.

First published November 25, 2019.

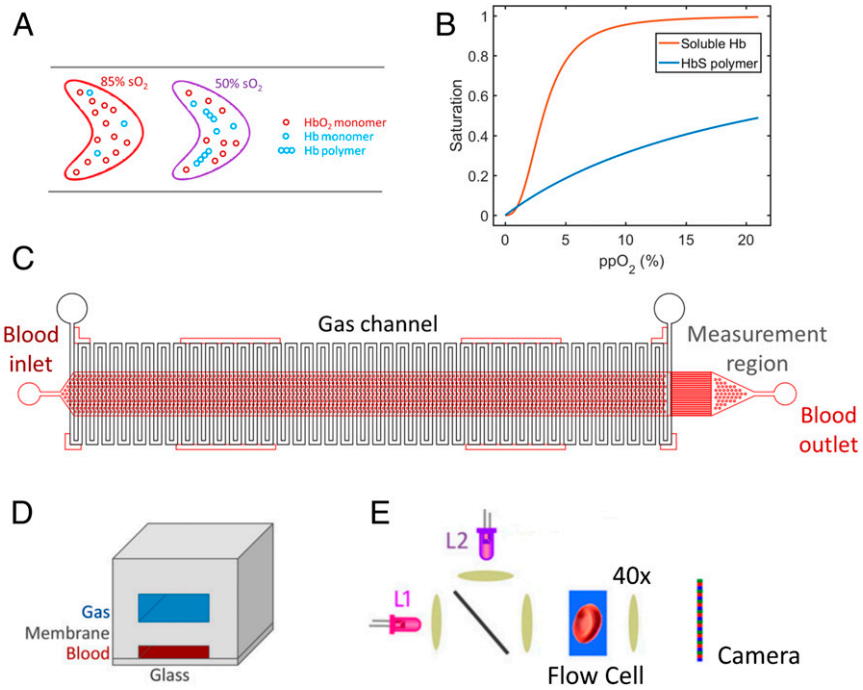

Fig. 1. Inferring single-RBC hemoglobin (Hb) polymer content from measurements of single-RBC hemoglobin-oxygen saturation. (*A*) The method is based on the principle that RBCs with less Hb polymer will have a higher fraction of their Hb saturated with oxygen than RBCs with more Hb polymer at a given oxygen tension. The cell on the left has less polymer, and 85% of its Hb is oxygen-saturated, while the cell on the right has more Hb polymer, and only 50% of its Hb is oxygen-saturated. *B* shows the hemoglobin-oxygen dissociation curves for soluble Hb (red), which demonstrates cooperativity, and polymerized Hb which is not cooperative (blue). The normal range of p50, the oxygen tension at which 50% of the Hb is oxygen-saturated, for soluble hemoglobin is ~3.1 to 3.7%, in contrast to Hb polymer which has p50 of ~22%. (*C*) The microfluidic device schematic shows the gas channel deoxygenation region (vertical white serpentine channels) and the blood channels (red horizontal channels) where cytometric measurements are performed at the rightmost end. *D* shows the cross-section of the device's 3 layers, and *E* shows the optical measurement setup: 2 LEDs (λ_{L1} = 410 nm and λ_{L2} = 430 nm) are combined using a nonpolarizing beam splitter. The light transmitted by the cells flowing in the microfluidic channel is then projected onto a color camera by a microscope objective. See ref. 10 for more details of the optical method.

containing low amounts of Hb polymer (12). An RBC's oxygen saturation is therefore inversely proportional to the amount of Hb polymer it contains, as previous investigators have noted (13, 14). As oxygen tension drops, increasing numbers of HbS molecules release oxygen, and the probability of polymer formation increases. Hb polymer does have some oxygen affinity. Fig. 1*B* shows the oxygen dissociation curves for hemoglobin monomer and hemoglobin polymer and illustrates that polymerized hemoglobin (p50 ~22%) has dramatically lower oxygen affinity than soluble hemoglobin (p50 ~3.7%) except in near anoxic conditions (15). By measuring the oxygen saturation of individual RBCs, it is possible to infer the amount of Hb polymer in each RBC. In this work, we demonstrate the application of this principle to characterize the single-RBC distribution of Hb polymer in populations of RBCs in patient blood samples. We compare these single-RBC polymer distributions at different oxygen tensions and for 2 different SCD patients with different HbF fractions. We further show how these measurements can provide a personalized estimate of the threshold maximal oxygen tension below which a detectable fraction of RBCs in a particular patient's blood sample will form significant amounts of hemoglobin polymer.

Materials and Methods

Measuring the Oxygen Saturation of Single RBCs. Oxygen saturation of single RBCs is determined using a previously reported quantitative absorptive cytometer (QAC) that measures oxygenated and deoxygenated hemoglobin in individual RBCs by quantifying the attenuation of light at 2 different wavelengths, 410 and 430 nm (10, 11). Briefly, RBCs are suspended in a 20% albumin buffer at physiological pH and maintained at ambient oxygen tension prior to imaging in a microfluidic flow chamber on a microscope at physiologic temperature (37^0 C). Blood samples were obtained under a discarded specimen research protocol approved by the Partners Healthcare Institutional Review Board (IRB). The microfluidic device is shown in Fig. 1 *C* and *D* and contains a 3-cm-long gas exchange region (Fig. 1*C*) enabling control of oxygen tension (Fig. 1*D*). A pressure gradient is applied such that RBCs traverse the channel in ~15 s. On exiting the gas region, RBCs are imaged at 2 wavelengths (Fig. 1*E*), enabling quantification of the oxygenated hemoglobin mass and deoxygenated hemoglobin mass using each species' known extinction coefficient (10). The ratio of oxygenated to total hemoglobin provides each RBC's percent hemoglobin-oxygen saturation. At each oxygen tension in the results reported below, approximately 1,000 RBCs are measured. See *Supplementary Information*, *Supplementary Methods* and *Supplementary Results* for more detail. Fig. 2*A* shows a hemoglobin-oxygen saturation distribution for a population of RBCs containing nonsickle hemoglobin (HbA) at 5.9% oxygen tension. For all RBCs in this blood sample, about 80% of the hemoglobin is oxygenated, with little variation from one RBC to the next. The same measurement can be made for RBCs containing HbS to infer the presence of Hb polymer.

Materials and Data Availability. All experimental protocols, including device fabrication details, are described in prior publications (10, 11, 16), *Materials and Methods*, or *Supplementary Information*. Data associated with patient specimens that can be shared under our IRB Protocol are included in *Results* or *Supplementary Information*.

Results

Single-RBC Oxygen Saturation Distributions Reveal Single-RBC Hb Polymer Distributions. At intermediate oxygen tension (~2% to ~8%), the single-RBC saturation distribution for blood samples containing HbS can be bimodal. Fig. 2*B* shows a saturation distribution for an SCD blood sample with 82% HbS, 14% HbF, and 4% HbA2 at 5.9% oxygen. There is one large peak at higher saturation with a mean saturation of about 80%, comparable to

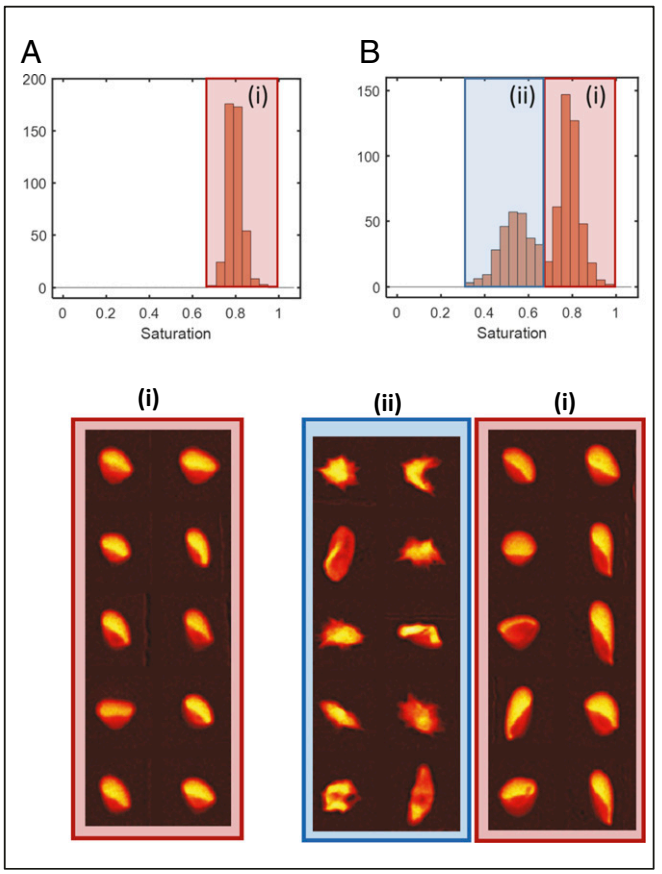

Fig. 2. Single-RBC oxygen saturation distributions reflect Hb polymer content. (*A*) A normal HbA blood sample at 5.9% oxygen contains RBCs with a unimodal saturation distribution clustered around ∼80% saturation, and fraction *i* below shows that all representative RBCs have normal morphology. In contrast, the RBCs in a blood sample in *B* from a patient with SCD have a bimodal saturation distribution at 5.9% oxygen tension, with a lower saturation peak around ∼50% saturation and a higher saturation peak around ∼80%. Representative RBCs from the lower saturation peak (*ii*) have a distorted and sickled morphology consistent with the presence of significant Hb polymer in all RBCs, while representative RBCs from the higher saturation peak (*i*) have mostly normal morphology.

the typical saturation seen for the HbA-containing RBCs at this oxygen tension in Fig. 2*A*. There is a second peak at a lower saturation, with a mean around 50%. The appearance of this lower saturation peak can be explained by the presence of a subpopulation of RBCs that has formed sufficient Hb polymer at 5.9% oxygen that each RBC's overall oxygen saturation has dropped, falling below what is seen for RBCs containing no Hb polymer, for instance the HbA-containing RBCs in Fig. 2*A*. Representative RBCs sampled from the 2 peaks are shown in Fig. 2. The higher saturation peak includes RBCs with a mostly normal morphology, similar to those from Fig. 2*A*, with the "parachute" or "slipper" shape commonly found for HbA-containing RBCs in flow (17), suggesting that little or no Hb polymer is present in these RBCs. The lower saturation peak includes RBCs with a mostly distorted morphology, suggesting the presence of significant polymer. It is important to note that morphology can be an insensitive and nonspecific marker of the presence of polymer, and it is possible that some RBCs with normal morphology contain polymer and that some RBCs with distorted morphology do not contain polymer (18, 19). Cellular hemoglobin-oxygen saturation is likely to be a more sensitive and specific marker of the presence of polymer, but investigation of cellular morphology is useful for qualitative validation. With no existing accepted measurement of single-RBC Hb polymer mass, it is difficult to calibrate an exact quantification of the Hb polymer mass in each RBC. The kinetics of sickle hemoglobin polymerization inside RBCs in vitro and in vivo are complex and clinically relevant (19–23). Some prior studies suggest that most polymers will have formed during the ∼15 s prior to measurement when cells are completely deoxygenated (20). This initial method is not designed to investigate these complicated polymerization kinetics, but it can be used to identify subpopulations of RBCs with a significantly increased amount of polymer relative to other RBCs in the population at the time of measurement. This method thus provides a semiquantitative measurement of Hb polymer in a population of RBCs and demonstrates at a single-RBC level what previous investigators reported for RBC populations: The amount of hemoglobin polymer is inversely proportional to the oxygen saturation (13, 14). We can then use the method to compare the saturation distributions and their subpopulations for blood samples from different SCD patients as a function of oxygen tension.

Single-RBC Oxygen Saturation Distributions Allow Comparison of Single-RBC Hb Polymer Distributions for Different Patients. The traditional hemoglobin-oxygen dissociation curves can be recreated by calculating the mean of the single-RBC saturation distribution under different oxygen tensions. Fig. 3*A* shows the mean hemoglobin saturation and single-RBC saturation distributions at 6 different oxygen tensions for RBCs from a healthy HbA blood sample (H). As expected, the oxygen saturation of a typical HbA RBC falls with decreasing oxygen and generally follows the expected sigmoid curve reflecting the cooperative binding of oxygen by hemoglobin. The single-RBC saturation histograms in Fig. 3*A* show that there is some heterogeneity in the measured saturation of individual RBCs at each fixed oxygen tension. Prior analysis suggests that most of this variation is biological as opposed to measurement noise (10). The heterogeneity in single-RBC saturation in the HbA sample seems to reach a maximum near the steepest part of the hemoglobin-oxygen dissociation curve around 2.5 to 4.5%. Fig. 3 *B* and *C* show RBC saturation means and distributions for blood samples from 2 different SCD patients (SS1 with 74% HbS, 21% HbF, and 5% HbA2; and SS2 with 82% HbS, 14% HbF, and 4% HbA2). Both SCD blood samples have bimodal saturation distributions at intermediate oxygen tensions.

While the mean saturations for the SCD samples are only slightly lower than those for the HbA sample at intermediate oxygen tensions, the single-RBC saturation distributions have markedly different shapes. There is a distinct second peak at a lower saturation when oxygen tension is in the intermediate range (∼2–8%). As shown above in Fig. 2, the RBCs in the lower-saturation peak would be expected to have more Hb polymer to explain their lower saturation, and their morphology is consistent with that expectation (Fig. 2). The higher-saturation peaks have oxygen saturations similar to those of the healthy control at the same oxygen pressure, consistent with a much lower amount of Hb polymer in those RBCs. The separation between the 2 peaks along the saturation axis decreases as oxygen tension is lowered until the 2 peaks nearly merge at 2.5% or below, where the saturation for hemoglobin polymer is no longer expected to be significantly different from that for hemoglobin monomer (Fig. 1*B*).

Fig. 3 *B* and *C* also show that the 2 SCD samples differ in terms of the sizes of their lower saturation peaks at each intermediate oxygen tension. Sample SS1 has fewer RBCs in the lower-saturation peak. In other words, at each intermediate oxygen tension, SS1 appears to have fewer RBCs with significant amounts of polymer than SS2. SS1 also has a higher fetal hemoglobin fraction. A higher level of HbF in an individual RBC will reduce the probability of polymerization at a given oxygen

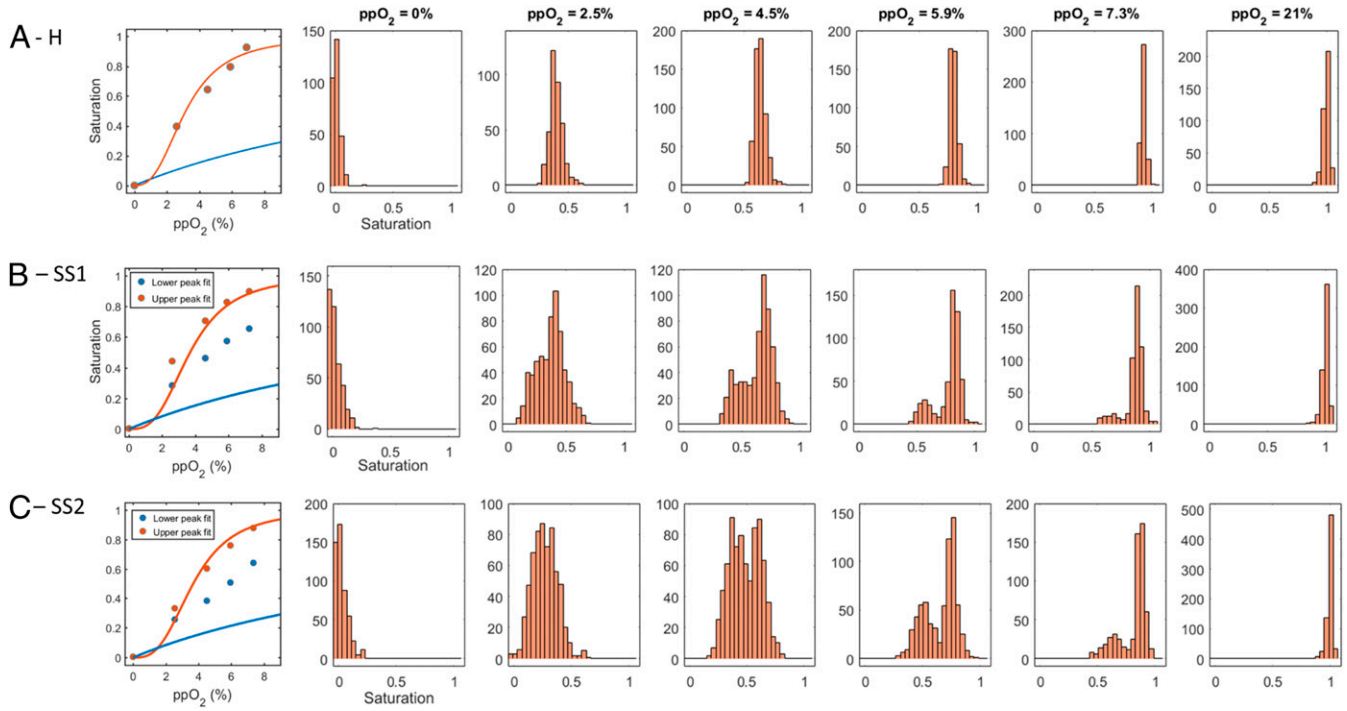

Fig. 3. Single-RBC saturation distributions reveal large differences in RBC subpopulations despite modest differences in mean saturations. *A* shows mean single-RBC hemoglobin saturation as a function of oxygen (dots in *Left*) and single-RBC saturation histograms for a healthy HbA sample (*H*) at 6 different oxygen tensions. *B* shows the same plots for a sickle cell sample (SS1) with 74% HbS, 21% HbF, and 5% HbA2. The mean saturations as function of oxygen tension are only modestly shifted downward relative to the dots in *A*, *Left* for sample H. The shapes of the histograms in *B* are markedly different from those in *A* at the intermediate oxygen tensions, with 2 modes instead of 1. The dots in *Left* show means of the upper and lower peaks of the saturation distributions at each measured oxygen tension. The saturations in the upper peaks are generally consistent with those in sample H, while the saturations in the lower peak are intermediate between those of sample H and what is expected for pure hemoglobin polymer as shown by the blue curve in the leftmost panel. (See Fig. 4 for more detail on fits used to define upper and lower peaks.) *C* shows results for another sickle cell sample (SS2) with 82% HbS, 14% HbF, and 4% HbA2. The dots in the leftmost panel show means of the upper and lower peaks of the saturation distributions at each measured oxygen tension as in *B*. At intermediate oxygen tensions (4.5, 5.9, and 7.3%) both SCD samples show a bimodal oxygen saturation distribution as described above and in Fig. 2, but the relative sizes of the 2 populations vary with oxygen tension and vary between patients. The curves in *Left* in each row also show the typical hemoglobin-oxygen dissociation curve for monomeric (red) and polymeric (blue) Hb.

tension (3–6). Differences in the distribution of HbF across RBCs may therefore explain the measured differences in the sizes of the lower saturation peaks for SS1 and SS2.

An RBC's overall saturation is determined by the relative fractions of polymer and monomer it contains and will equal the pure monomeric and polymeric saturations weighted by those fractions. Accurate inference of polymer fraction for an RBC therefore requires validated standard curves for the saturations of pure monomer and polymer under conditions identical to those of the particular RBC in our measurement system, including the RBC's oxygenation history, its intracellular hemoglobin concentration, its HbF fraction, and more. Accurate standard curves are not available, but we can use the standard curves previously reported under other conditions to estimate a polymer fraction for the typical RBC in the low saturation peak for each blood sample as a function of oxygen tension. For both samples, at 7.3%, when the typical high peak RBC is about 80% saturated, the average RBC in the low peak may have a ~1/3 polymer fraction. The inferred polymer fraction increases toward 1/2 as oxygen drops, but uncertainties in the precision of standard curves become more significant as the curves begin to merge below ~4% oxygen. This estimated polymer fraction of about 1/3 at an oxygen tension of 7.3% and a monomeric or solution phase saturation of about 80%, and a further increase in polymer fraction toward 1/2 as oxygen level decreases, are consistent with what has been measured (23, 24) and theoretically predicted (19, 24, 25) by previous investigators.

Heterogeneity in Single-RBC Saturation Distributions Is Associated with Patient HbF Fraction. It is clear that the single-RBC saturations distributions for SCD RBCs are far more heterogeneous than those for HbA RBCs which will not form polymer (Fig. 3). Further analysis of this distributional heterogeneity can also highlight differences between SCD samples that govern polymer formation and may ultimately be clinically relevant. One metric to quantify this heterogeneity is an estimate of the size of the fraction of RBCs in the lower-saturation peaks, which can be obtained, for instance, by fitting the saturation distributions to a mixed Gaussian statistical model. Fig. 4 shows the saturation distributions and corresponding mixed Gaussian fits for both SCD samples at 3 intermediate oxygen tensions. At oxygen tensions below 4.5% and above 7.3%, the distributions are close to unimodal, and fits are not shown. The lower saturation peaks for SS2 (Fig. 4*B*) are larger than for SS1 (Fig. 4*A*) at all intermediate oxygen tensions. As noted above, this ordering is consistent with what would be expected given that SS1 had a higher HbF fraction, which would tend to reduce Hb polymer formation (3–6). For both SCD samples, the estimated lower saturation peak sizes increase roughly linearly with decreasing oxygen (Fig. 4*C*). If the linear curves are extrapolated to higher oxygen tension, we can estimate the highest oxygen tension at which some RBCs in each blood sample will first begin to form sufficient Hb polymer to alter the RBC oxygen saturation. For SS1, this extrapolation method estimates that polymerization first begins at oxygen tensions below ~9%, and for SS2 we estimate that polymerization first begins at oxygen tensions below ~10.5%. The lower estimated

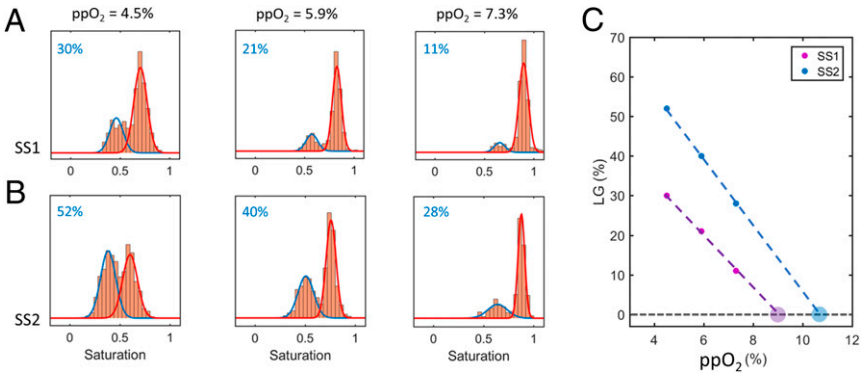

Fig. 4. Mixed Gaussian fits of single-RBC oxygen saturation distributions enable estimation of the size of the lower-saturation peaks and extrapolation to a patient-specific threshold oxygen tension below which polymerization may begin. *A* and *B* show the saturation distributions of both SCD samples at 3 intermediate oxygen tensions. The distributions have a bimodal shape and are shown along with the results of a mixed Gaussian fit. Each plot also shows (in blue) the fitted proportion of RBCs that falls in the lower saturation peak. *C* shows the percentage of cells in the lower Gaussian (LG) peak as a function of oxygen tension for both samples. The larger filled circles represent the *x*-intercept of a linear fit through the data of each sample.

hemoglobin polymerization threshold for SS1 is consistent with its higher HbF fraction. Both of these estimated polymerization thresholds are within the range of oxygen tensions typically found in the arterial circulation, consistent with prior studies of the oxygen dependence of polymer formation and blood rheology (26–28).

Another simpler way to quantify the heterogeneity in the oxygen saturation distributions is to compare the second and fourth quintiles of the saturation distributions (the 20th and 80th percentile saturations). The difference in saturation between the 20th and 80th percentiles ("quintile metric") at each oxygen tension is shown in Fig. 5*A* for each of the 3 blood samples. Sample H has a relatively narrow saturation distribution across the full range of oxygen tensions, and the quintile metric reaches a maximum at only 5% when the oxygen tension is already low (~2.5%). Samples SS1 and SS2 have more heterogeneity than sample H according to this metric at all but the highest oxygen tension, where they are the same. Sample SS2 reaches the highest maximum of the 3 samples (19% at 5.9% oxygen), which is consistent with its lower HbF level compared to SS1. Interestingly, sample SS2 shows maximal heterogeneity at an oxygen tension above its p50, where the typical RBC contains more than 50% oxygenated hemoglobin, suggesting that even when SS2 blood is more than 50% oxygen-saturated, a large fraction of RBCs contains significant polymer.

We expect to find more Hb polymer in more RBCs in the second quintile as compared to RBCs in the fourth quintiles. Fig. 5*B* shows images of randomly chosen RBCs from the second and fourth quintiles for all 3 samples at 5.9% oxygen tension. For sample H, the typical RBC morphology is normal in both quintiles, with the "parachute" or "slipper" shape commonly found for RBCs in flow (17). For SS1, the majority of RBCs from the second quintile are deformed consistent with the presence of polymer, and almost all of those in the fourth quintile have normal-appearing morphology. For SS2, RBCs from the second quintile are almost uniformly deformed consistent with the presence of polymer, and the majority of those in the fourth quintile have normal-appearing morphology. These RBC images support the conclusion that the lower saturation peaks in the SCD saturation distributions are associated with increased Hb polymerization in a subpopulation of RBCs, and a comparison of distribution quintiles provides one simple quantification of the heterogeneity of a blood sample's saturation distributions in a way that appears to be consistent with that sample's overall propensity for and extent of polymerization.

Discussion

We describe a semiquantitative method to compare the single-RBC distributions of Hb polymer determined by differential

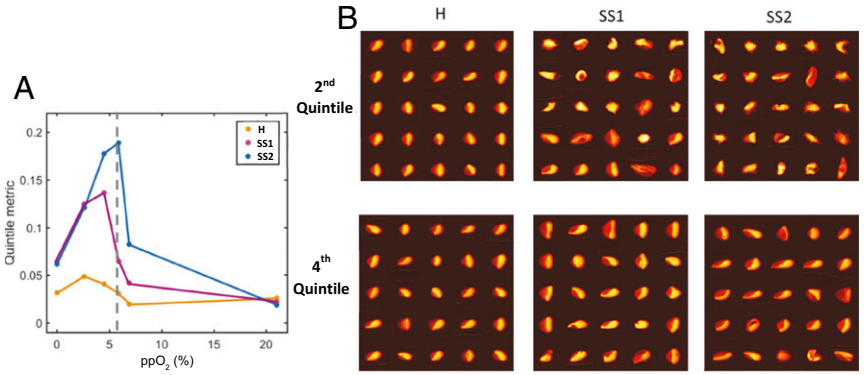

Fig. 5. Measuring RBC saturation distribution heterogeneity by comparing quintiles. (*A*) The difference between the 80th and 20th percentiles ("Quintile metric") of the single-RBC saturation distributions (Fig. 3) is plotted for each of the 3 samples as a function of oxygen tension. The SCD samples have maximal values much higher than the healthy control sample. *B* shows the morphology of RBCs taken at random from the second and fourth quintiles at 5.9% oxygen. In the second quintile, a majority of the RBCs from SS1 have a morphology consistent with the presence of polymer, and several have normal-appearing morphology. For SS2, an even larger fraction of RBCs in the second quintile seem to have a morphology consistent with the presence of polymer. In the fourth quintile, the vast majority of RBCs have normal-appearing morphology for both SS1 and SS2.

oxygen affinity as a function of controlled oxygen tension for individual patients with SCD. We find that blood samples from 2 SCD patients show bimodal saturation distributions in the physiologic range of oxygen tension. The lower saturation peaks of these distributions appear to contain RBCs with significantly more Hb polymer than the higher saturation peaks, and the mean saturations are modestly reduced and still comparable to those of a blood sample containing HbA that will not polymerize. We show that the heterogeneity in the oxygen saturation distributions can be quantified using multiple metrics to distinguish individuals with SCD from individuals with HbA blood, and the heterogeneity in the saturation distributions also reveals apparent SCD patient-specific differences in polymer formation patterns that may correlate with HbF levels. Future development of the platform would include further calibration of the method with a goal of providing absolute quantification of the mass or concentration of Hb polymer in each RBC. Future studies are needed to confirm that the patterns of association between RBC saturation distributions and bulk HbF fractions persist, and to determine associations between saturation distributions and specific patient clinical outcomes.

This study also motivates follow-up investigation to understand in greater detail the mechanisms for the bimodality of SCD saturation distributions at intermediate oxygen tension. Based on work by prior investigators (13, 14), we would expect deoxygenation to shift the lower saturation tails of saturation distributions to the left as polymer forms in individual RBCs and lowers their oxygen saturation. It is not clear that the observed jump down in saturation leading to a second peak would be expected. Prior studies of RBCs at the population level reported a more continuous increase in polymer fraction with decreasing oxygen tension (19, 24), but single-cell studies of polymer fraction are not available. The bimodality may be consistent with prior reports of the sigmoidal polymerization progression function (29, 30). The lower saturation peak grows with decreasing oxygen tension, making clear that more and more RBCs are forming significant amounts of polymer at lower oxygen tensions.

A fully quantitative and calibrated measurement of single-RBC polymer mass and fraction would help reveal the mechanisms for the observed bimodality and would also allow exploration of the role of sickle hemoglobin polymerization kinetics. Our results were measured after a constant duration of exposure to controlled oxygen, about 15 s. The kinetics of sickle hemoglobin polymerization are known to be complex and influenced by factors such as hemoglobin isoform concentration, hydroxyurea treatment, cell volume, and more (20, 21, 23, 31). Future study with a fully quantitative measurement made at multiple oxygen exposure times, and ideally measuring saturation repeatedly for the same individual RBCs, is necessary to explore contributions of polymerization kinetics to bimodality and to other aspects of the results presented here. An alternative approach for investigating polymer fractions as a function of oxygen tension independent of polymerization kinetics would be to measure single-cell saturation distributions of RBCs that were first equilibrated under anoxic conditions, thereby starting in the maximally polymerized state and allowing comparison of the effects of complicated polymerization kinetics with the less complicated depolymerization kinetics (32, 33). The current system uses a refractive index-matched buffer to limit noise from extracellular optical scattering, but intracellular scattering is not eliminated, and future enhancements will also explore the use of additional illumination wavelengths to provide an opportunity to reduce noise even further (16).

The current absence of an assay that can accurately quantify the level of HbF in individual RBCs (3, 34) has likely constrained the development of effective treatments for SCD over the past few decades. Given recent progress with genetic approaches to treatment (7–9), some of which induce expression of synthetic hemoglobin isoforms that inhibit polymerization, a measurement of single-RBC Hb polymer would seem to be more useful than a measurement of single-RBC HbF. A measurement of single-RBC polymer would also appear to have advantages for these purposes over sickling assays or other morphology-based assessments that are limited by the uncertain relationship between morphology and polymer content (18, 19). Single-cell saturation measurements may help rationalize differences in clinical course for patients with other sickling syndromes including hemoglobin SC disease and sickle-beta-plus and sickle-beta-zero thalassemia. This approach also has the potential to accelerate diagnostic and treatment development. The ability to resolve polymerization in a small subset of cells may enable clearer comparison of the efficacy of different therapies in development and in use, including experimental approaches designed to increase hemoglobin oxygen affinity or to up-regulate fetal hemoglobin. This method also raises the possibility of providing objective patient-specific endpoints defined in terms of single-RBC polymer distributions for treatment with simple or exchange blood transfusion.

ACKNOWLEDGMENTS. Portions of this work were conducted in the Minnesota Nano Center, which is supported by the National Science Foundation through the National Nano Coordinated Infrastructure Network under Award ECCS-1542202. This work was supported by National Heart, Lung, and Blood Institute Grants HL130818 and HL132906. We thank Chhaya Patel and Hasmukh Patel for assistance with blood sample collection, Carlo Brugnara and Frank Bunn for helpful discussions, and the editor and 2 anonymous reviewers for helpful comments and suggestions.

1. G. R. Serjeant, D. R. Higgs, I. R. Hambleton, Elderly survivors with homozygous sickle cell disease. *N. Engl. J. Med.* **356**, 642–643 (2007).
2. R. Kalpatthi, E. M. Novelli, Measuring success: Utility of biomarkers in sickle cell disease clinical trials and care. *Hematology Am Soc Hematol Educ Program* **2018**, 482–492 (2018).
3. M. H. Steinberg, D. H. K. Chui, G. J. Dover, P. Sebastiani, A. Alsultan, Fetal hemoglobin in sickle cell anemia: A glass half full? *Blood* **123**, 481–485 (2014).
4. S. Charache *et al.*; Investigators of the Multicenter Study of Hydroxyurea in Sickle Cell Anemia, Effect of hydroxyurea on the frequency of painful crises in sickle cell anemia. *N. Engl. J. Med.* **332**, 1317–1322 (1995).
5. O. S. Platt *et al.*, Pain in sickle cell disease. Rates and risk factors. *N. Engl. J. Med.* **325**, 11–16 (1991).
6. O. S. Platt *et al.*, Mortality in sickle cell disease. Life expectancy and risk factors for early death. *N. Engl. J. Med.* **330**, 1639–1644 (1994).
7. J. A. Ribeil *et al.*, Gene therapy in a patient with sickle cell disease. *N. Engl. J. Med.* **376**, 848–855 (2017).
8. E. B. Esrick *et al.*, Flipping the switch: Initial results of genetic targeting of the fetal to adult globin switch in sickle cell patients. *Blood* **132**, 1023 (2018).
9. J. F. Tisdale *et al.*, Current results of lentiglobin gene therapy in patients with severe sickle cell disease treated under a refined protocol in the phase 1 Hgb-206 study. *Blood* **132**, 1026 (2018).
10. G. Di Caprio, C. Stokes, J. M. Higgins, E. Schonbrun, Single-cell measurement of red blood cell oxygen affinity. *Proc. Natl. Acad. Sci. U.S.A.* **112**, 9984–9989 (2015).
11. E. Schonbrun, R. Malka, G. Di Caprio, D. Schaak, J. M. Higgins, Quantitative absorption cytometry for measuring red blood cell hemoglobin mass and volume. *Cytometry A* **85**, 332–338 (2014).
12. W. A. Eaton, H. F. Bunn, Treating sickle cell disease by targeting HbS polymerization. *Blood* **129**, 2719–2726 (2017).
13. R. E. Benesch, R. Edalji, S. Kwong, R. Benesch, Oxygen affinity as an index of hemoglobin S polymerization: A new micromethod. *Anal. Biochem.* **89**, 162–173 (1978).
14. M. E. Fabry, L. Desrosiers, S. M. Suzuka, Direct intracellular measurement of deoxygenated hemoglobin S solubility. *Blood* **98**, 883–884 (2001).
15. A. Mozzarelli, C. Rivetti, G. L. Rossi, E. R. Henry, W. A. Eaton, Crystals of haemoglobin with the T quaternary structure bind oxygen noncooperatively with no Bohr effect. *Nature* **351**, 416–419 (1991).
16. E. Schonbrun, G. Di Caprio, D. Schaak, Dye exclusion microfluidic microscopy. *Opt. Express* **21**, 8793–8798 (2013).
17. R. Skalak, P. I. Branemark, Deformation of red blood cells in capillaries. *Science* **164**, 717–719 (1969).
18. H. Hiruma *et al.*, Sickle cell rheology is determined by polymer fraction–Not cell morphology. *Am. J. Hematol.* **48**, 19–28 (1995).
19. W. A. Eaton, J. Hofrichter, Hemoglobin S gelation and sickle cell disease. *Blood* **70**, 1245–1266 (1987).
20. K. R. Bridges *et al.*, A multiparameter analysis of sickle erythrocytes in patients undergoing hydroxyurea therapy. *Blood* **88**, 4701–4710 (1996).
21. F. A. Ferrone, J. Hofrichter, H. R. Sunshine, W. A. Eaton, Kinetic studies on photolysis-induced gelation of sickle cell hemoglobin suggest a new mechanism. *Biophys. J.* **32**, 361–380 (1980).

22. A. Mozzarelli, J. Hofrichter, W. A. Eaton, Delay time of hemoglobin S polymerization prevents most cells from sickling in vivo. *Science* **237**, 500–506 (1987).
23. H. R. Sunshine, J. Hofrichter, F. A. Ferrone, W. A. Eaton, Oxygen binding by sickle cell hemoglobin polymers. *J. Mol. Biol.* **158**, 251–273 (1982).
24. C. T. Noguchi, D. A. Torchia, A. N. Schechter, Determination of deoxyhemoglobin S polymer in sickle erythrocytes upon deoxygenation. *Proc. Natl. Acad. Sci. U.S.A.* **77**, 5487–5491 (1980).
25. W. A. Eaton, J. Hofrichter, Sickle cell hemoglobin polymerization. *Adv. Protein Chem.* **40**, 63–279 (1990).
26. G. M. Brittenham, A. N. Schechter, C. T. Noguchi, Hemoglobin S polymerization: Primary determinant of the hemolytic and clinical severity of the sickling syndromes. *Blood* **65**, 183–189 (1985).
27. T. Itoh, S. Chien, S. Usami, Deformability measurements on individual sickle cells using a new system with pO2 and temperature control. *Blood* **79**, 2141–2147 (1992).
28. X. Lu, D. K. Wood, J. M. Higgins, Deoxygenation reduces sickle cell blood flow at arterial oxygen tension. *Biophys. J.* **110**, 2751–2758 (2016).
29. F. A. Ferrone, The delay time in sickle cell disease after 40 years: A paradigm assessed. *Am. J. Hematol.* **90**, 438–445 (2015).
30. M. Ivanova, R. Jasuja, S. Kwong, R. W. Briehl, F. A. Ferrone, Nonideality and the nucleation of sickle hemoglobin. *Biophys. J.* **79**, 1016–1022 (2000).
31. Q. Li *et al*., Kinetic assay shows that increasing red cell volume could be a treatment for sickle cell disease. *Proc. Natl. Acad. Sci. U.S.A.* **114**, E689–E696 (2017).
32. K. Moffat, Q. H. Gibson, The rates of polymerization and depolymerization of sickle cell hemoglobin. *Biochem. Biophys. Res. Commun.* **61**, 237–242 (1974).
33. J. Hofrichter, P. D. Ross, W. A. Eaton, Kinetics and mechanism of deoxyhemoglobin S gelation: A new approach to understanding sickle cell disease. *Proc. Natl. Acad. Sci. U.S.A.* **71**, 4864–4868 (1974).
34. G. J. Dover, S. H. Boyer, Quantitation of hemoglobins within individual red cells: Asynchronous biosynthesis of fetal and adult hemoglobin during erythroid maturation in normal subjects. *Blood* **56**, 1082–1091 (1980).